Confined Crystallization of Polymers within Nanopores

Guoming Liu[1,2], Alejandro J. Müller[3,4], and Dujin Wang[1,2*]*

[1] Beijing National Laboratory for Molecular Sciences, Institute of Chemistry, Chinese Academy of Sciences, Beijing 100190, China

[2] University of Chinese Academy of Sciences, Beijing 100049, China

[3] POLYMAT and Department of Polymers and Advanced Materials: Physics, Chemistry and Technology, Faculty of Chemistry, University of the Basque Country UPV/EHU, Paseo Manuel de Lardizabal, 3, 20018 Donostia-San Sebastián, Spain

[4] IKERBASQUE, Basque Foundation for Science, Bilbao, 48009, Spain

Corresponding author: alejandrojesus.muller@ehu.es, djwang@iccas.ac.cn

CONSPECTUS

Crystallization of polymeric materials under nanoscopic confinement is highly relevant for nanotechnology applications. When a polymer is confined within rigid nanoporous anodic aluminum oxide (AAO) templates, the crystallization behavior experiences dramatic changes as the pore size is reduced, including nucleation mechanism, crystal orientation, crystallization kinetics, and polymorphic transition, etc. As an experimental prerequisite, exhaustive cleaning procedures after infiltrations of polymers in AAO pores must be performed to ensure producing an ensemble of isolated polymer-filled nanopores. Layers of residual polymers on the AAO surface percolate nanopores and lead to the so-called "fractionated crystallization", i.e., multiple crystallization peaks during cooling.

As the density of isolated nanopores in a typical AAO template exceeds the density of heterogeneities in bulk polymers, the majority of nanopores will be heterogeneity-free. This means that the nucleation will proceed by surface or homogeneous nucleation. As a consequence, a very large supercooling is necessary for crystallization, and its kinetics is reduced to a first-order process that is dominated by nucleation. Self-nucleation is a powerful method to exponentially increase nucleation density. However, when the diameter of the nanopores is lower than a critical value, confinement prevents the possibility to self-nucleate the material.

Because of the anisotropic nature of AAO pores, polymer crystals inside AAO also exhibit anisotropy, which is determined by thermodynamic stability and kinetic selection rules. For low molecular weight poly(ethylene oxide) (PEO) with extended chain crystals, the orientation of polymer crystals changes from the "chain perpendicular to" to "chain parallel to" AAO pore axis, when the diameter of AAO decreases to the contour length of the PEO, indicating the effect of

thermodynamic stability. When the thermodynamic requirement is satisfied, the orientation is determined by kinetics including crystal growth, nucleation and crystal growth rate. An orientation diagram has been established for PEO/AAO system, considering the cooling condition and pore size.

The interfacial polymer layer has different physical properties as compared to the bulk. In poly(L-lactic acid), the relationship between the segmental mobility of the interfacial layer and crystallization rate is established. For the investigation of polymorphic transition of poly(butane-1), the results indicate that a 12 nm interfacial layer hinders the transition of Form II to Form I. Block and random copolymers have also been infiltrated into AAO nanopores, and their crystallization behavior is analogously affected as pore size is reduced.

KEY REFERENCES

- Guan, Y.; Liu, G.; Gao, P.; Li, L.; Ding, G.; Wang, D., Manipulating Crystal Orientation of Poly(ethylene oxide) by Nanopores. *ACS Macro Letters* **2013**, 2, 181-184.[1] *The orientation of a low molecular weight PEO changes when the diameter of AAO approaches the counter length of the PEO extended chain crystal, indicating the decisive effect of thermodynamic stability on crystal orientation.*
- Shi, G.; Liu, G.; Su, C.; Chen, H.; Chen, Y.; Su, Y.; Müller, A. J.; Wang, D., Reexamining the Crystallization of Poly(ε-caprolactone) and Isotactic Polypropylene under Hard Confinement: Nucleation and Orientation. *Macromolecules* **2017**, 50, 9015-9023.[2] *Fractionated crystallization of confined polymers in AAO is explained by the residual polymers on the AAO surface. The importance of surface cleaning is emphasized, providing a general experimental guideline to the study of confined crystallization using templates.*

- Su, C.; Shi, G.; Li, X.; Zhang, X.; Müller, A. J.; Wang, D.; Liu, G., Uniaxial and Mixed Orientations of Poly(ethylene oxide) in Nanoporous Alumina Studied by X-ray Pole Figure Analysis. *Macromolecules* **2018**, 51, 9484-9493.[3] *A model is proposed to explain the orientation diagram of PEO, illustrating the role of nucleation and crystal growth rates and contributing to a complete understanding of crystal orientation.*
- Shi, G.; Guan, Y.; Liu, G.; Müller, A. J.; Wang, D., Segmental Dynamics Govern the Cold Crystallization of Poly(lactic acid) in Nanoporous Alumina. *Macromolecules* **2019**, 52, 6904-6912.[4] *The relationship between crystallization and segmental mobility of PLLA chains at the polymer/AAO interface is established, which contributes to a general understanding of the impact of the interfacial layer.*

1. INTRODUCTION

Polymeric materials are ubiquitous in industry and in human life, among which 70% are semi-crystalline polymers. How a long flexible chain, frequently entangled with neighboring chains, crystallizes as crystals with three-dimensional order has been a puzzle. Till now, there is still a lack of a well-accepted crystallization theory that can explain all of the experimental phenomena.[5, 6] The duality of "commercial success" and "theoretical deficiency" has coexisted in this field for decades. The basic building block of polymer crystals is the two-dimensional folded-chain lamella with a typical thickness of ca. 10 nm. On this scale, metastable states and kinetics play a critical role in polymer crystallization.[7, 8]

With the blooming of nanoscience and nanotechnology, the physical properties of materials in very small dimensions have caught great attention because they deviate significantly from those of the bulk. How the crystallization behavior changes with decreasing size became a hot topic of research since the 1990s with the development of block copolymers.[9-13] Meanwhile, self-ordered porous anodic aluminum oxide templates (AAO) were fabricated to prepare organic or inorganic nanostructures.[14-17] AAO contains hexagonal arrays of nanopores that are parallel and separated by boundaries. The pore diameter is in the range of 10 ~ 400 nm, and the length of the pore ranges from tens to hundreds of micrometers.

Figure 1 shows the typical nanostructures prepared using AAO as templates, including platinum (Pt) arrays,[14] polystyrene (PS) nanotubes,[16] isotactic polypropylene (iPP) nanorods,[18] and poly(ε-caprolactone) (PCL) nanorods.[2] Geometrically, AAO pores are similar to the cylinder phase of block copolymers. Compared with block copolymers, the pores of AAO cover a broader range of diameter and length. More importantly, they are physically isolated, and there are no

chemical bonds at the interface. Thus, AAO templates provide a convenient model system to study the crystallization behavior of polymers under cylindrical confinement.

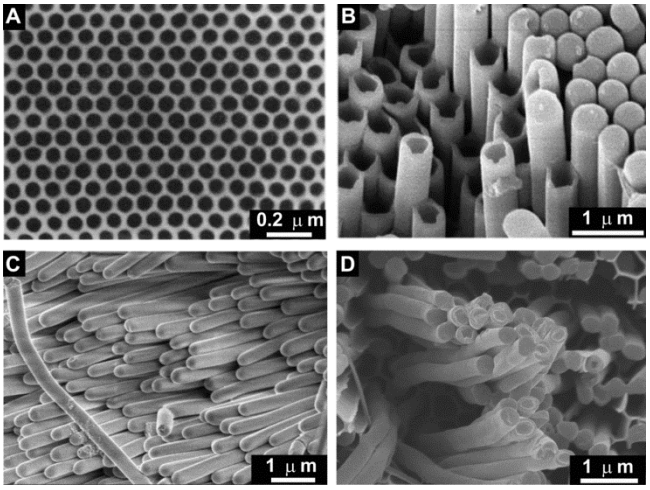

Figure 1. (A) Top image of Pt template prepared by using a two-step replica method of AAO,[14] (B) PS nanotubes,[16] (C) *i*PP rods,[18] and (D) PCL rods[2] prepared by AAO molding and subsequent dissolving the templates. Reproduced with permission from refs [14], [16], [18], and [2]. Copyright 1995, 2002 AAAS, Copyright 2011, 2017 American Chemical Society.

This account highlights the experimental results and understanding of the features of confined crystallization of semi-crystalline polymers in our group in a phenomenological view. Considering crystallization, the easiest experiment is to perform a differential scanning calorimetry (DSC) test, where crystallization temperature (T_c), melting temperature (T_m) and crystallization and melting enthalpies (ΔH_c *and* ΔH_m) can be determined. Most frequently, the T_m of polymers confined within AAO shows no change or a slight decrease, and the melting enthalpy, corresponding to the crystallinity, decreases when the diameter of AAO pore decreases.[13, 19] The most interesting observation is the variation in T_c. Figure 2 summarizes the T_c of bulk and infiltrated homopolymers within AAO, plotted as a function of their T_m values (measured during a DSC heating scan). Data are taken from the ref.[1, 2, 18, 20-37] The

dotted line represents the thermodynamic equilibrium condition, where $T_c = T_m$. Depending on the type of polymers, the bulk samples exhibit supercoolings ($\Delta T = T_m - T_c$) in the range of 15 ~ 60 ºC. The red points are the T_c values of infiltrated polymers within AAO templates (only the lowest T_c values are shown here if multiple crystallization peaks exist). A dramatic decrease of T_c, as compared to the bulk, in the order of ~ 50 ºC can be observed.

The depression of T_c is a general phenomenon in confined polymers and has been explained by the transition of the nucleation mechanism from heterogeneous nucleation to surface or homogeneous nucleation. It is well-known that under normal cooling conditions, crystallization of a bulk polymer is primarily nucleated by the heterogeneities that persist in the melt, such as impurities, catalyst residues, etc. Once nucleated, the crystallization proceeds to fill the space by the growth step. However, for polymers that are confined in microdomains, e.g., the case of AAO pores, the growth step is physically prohibited among adjacent domains. Because each microdomain has to nucleate inside itself, naturally, those pores free from heterogeneities must crystallize *via* surface or homogeneous nucleation, which occurs at lower T_c values to overcome a higher free energy barrier.[38]

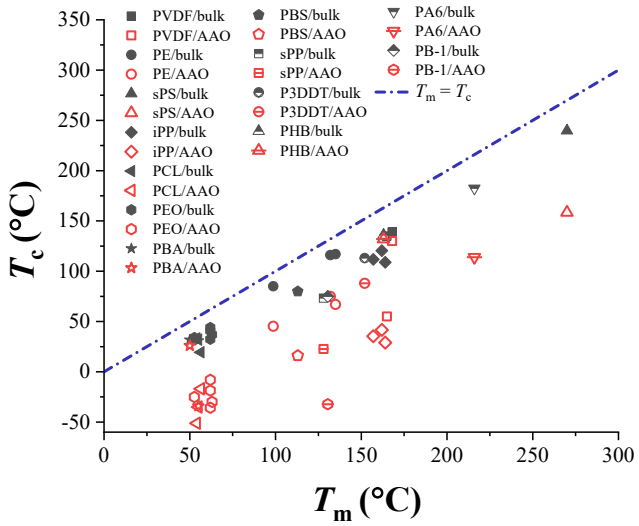

Figure 2. Crystallization temperature as a function of the melting temperature of different homopolymers infiltrated within AAO templates. The data points are taken from iPP,[2, 18, 20] PCL,[2, 21, 22] poly(vinylidene fluoride) (PVDF),[23, 24] polyethylene (PE),[25, 26] syndiotactic polystyrene (sPS),[27] poly(ethylene oxide) (PEO),[1, 26, 28-30] poly(butylene adipate) (PBA),[31, 32] poly(butylene succinate) (PBS),[32] syndiotactic polypropylene (sPP),[33] poly(3-dodecylthiophene) (P3DDT),[34] poly(3-hydroxybutyrate) (PHB),[35] polyamide 6 (PA6),[36] and poly(butene-1) (PB-1).[37]

2. FEATURES OF CONFINED CRYSTALLIZATION

2.1. Nature of Fractionated Crystallization

A frequently reported observation of polymer crystallization under confinement in AAO is the "fractionated crystallization", where "multiple crystallization peaks" were observed in a DSC cooling curve. Fractionated crystallization behavior has been reported in homopolymers, including PE,[25] iPP,[18, 20] sPS,[39] PCL,[21, 22] PEO,[28, 30] PVDF,[24] and copolymers such as PEO-*b*-PCL.[40] By intentionally placing a surface layer of PEO on top of the AAO template filled with PEO, we successfully observed an extra crystallization peak at a higher temperature, indicating a potential relationship between the surface layer and fractionated crystallization behavior.[41]

Motivated by the above peculiar experimental phenomenon, we systematically reexamined the crystallization behavior of PCL and iPP to clarify the nature of fractionated crystallization under confinement. By testing different cleaning procedures, the polymers were infiltrated into AAO templates without surface residue. Different from the previous results,[18, 20, 21] only one crystallization peak was observed for all the samples (Figures 3A, 3B). To elucidate the relationship between surface residue and fractionated crystallization, we studied the effect of the

surface cleaning procedure. Figures 3C, 3D show four DSC curves of samples that were cleaned with different methods. From sample 1 to sample 4, with increasing the cleaning effectiveness, the high-temperature exothermic peak vanished gradually. This proves unambiguously that the surface residue is the reason for the observed fractionated crystallization behavior in the investigated two polymers, and can be a general reason for other polymers.

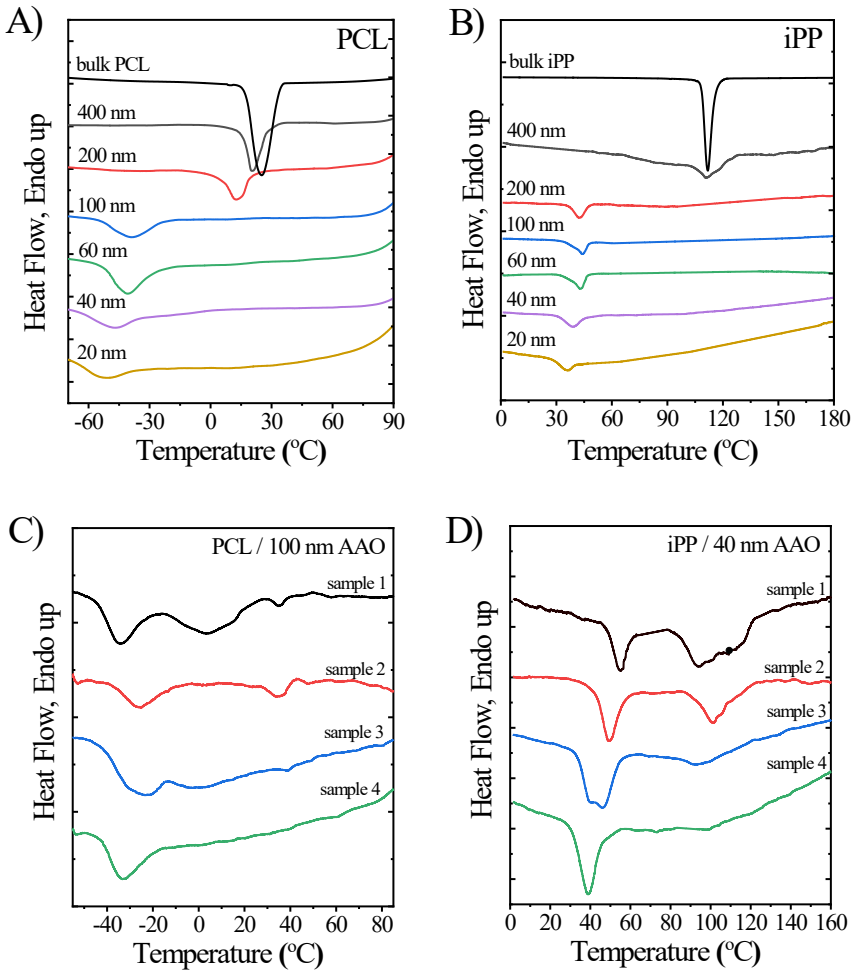

Figure 3. DSC cooling curves of bulk and infiltrated samples: (A) and (C) PCL, (B) and (D) iPP. For samples with different surface cleaning procedures, DSC cooling scans are shown in (C) and (D). The curves labeled with "sample 4" had no surface residue and showed only one exothermic

peak during cooling. Reproduced with permission from ref. [2]. Copyright 2017 American Chemical Society.

In fact, the origin of fractionated crystallization is already known in polymer blends.[42, 43] In an immiscible crystalline/amorphous blend, the crystalline polymer is dispersed in the amorphous matrix as microdomains if the crystalline polymer is the minor component. The heterogeneities that act as nuclei are also included in those microdomains (Figure 4, left-hand side). Here, "A" and "B" mean two different types of heterogeneities with different activities. Because the domains are physically isolated, a nucleus can only nucleate the microdomain that contains it. When a sample is cooled from the melt, the bulk sample is nucleated by "A" nuclei first, and the crystal spreads over to fill the space. On the other hand, if a blend with crystalline microdomains is cooled, the domains that contain "A" heterogeneities will crystallize first, resulting in the highest exothermic peak in DSC. The domains that contain "B" heterogeneities crystallize at a lower temperature. Finally, those heterogeneity-free domains crystallize at the lowest temperature *via* homogeneous nucleation or surface nucleation.

The key condition for fractionated crystallization is that the density of microdomains is in the same order of magnitude as the density of heterogeneities of the crystallizable polymer in the bulk, which is true in polymer blends. The typical heterogeneous nucleation density of a bulk polymer is $10^5 \sim 10^9$ cm^{-3}.[2] The size of the domain of a blend is typically 5 ~ 100 μm, corresponding to a number density of $10^6 \sim 10^{10}$ cm^{-3}. However, the typical density of AAO pores is in the range of $10^{11} \sim 10^{14}$ cm^{-3}, which is several orders of magnitude larger than that of heterogeneities in a polymer. Statistically, the majority of the AAO pores are heterogeneity-free. Therefore, fractionated crystallization in AAO must have other origins. A schematic is shown on the left-hand side of Figure 4. The highest crystallization peak that usually locates at a similar

temperature as that of the bulk is most probably caused by a large grain of residue that contains highly active heterogeneities and percolates a certain population of nanopores. The middle peak may be caused by the percolation of another group of nanopores by a thin surface layer. The lowest peak may be attributed to the heterogeneity-free pores. If the surface residue is cleaned by a proper method, only the lowest peak survives. The importance of surface cleaning must be emphasized because the presence of a surface layer may influence many aspects of crystallization.

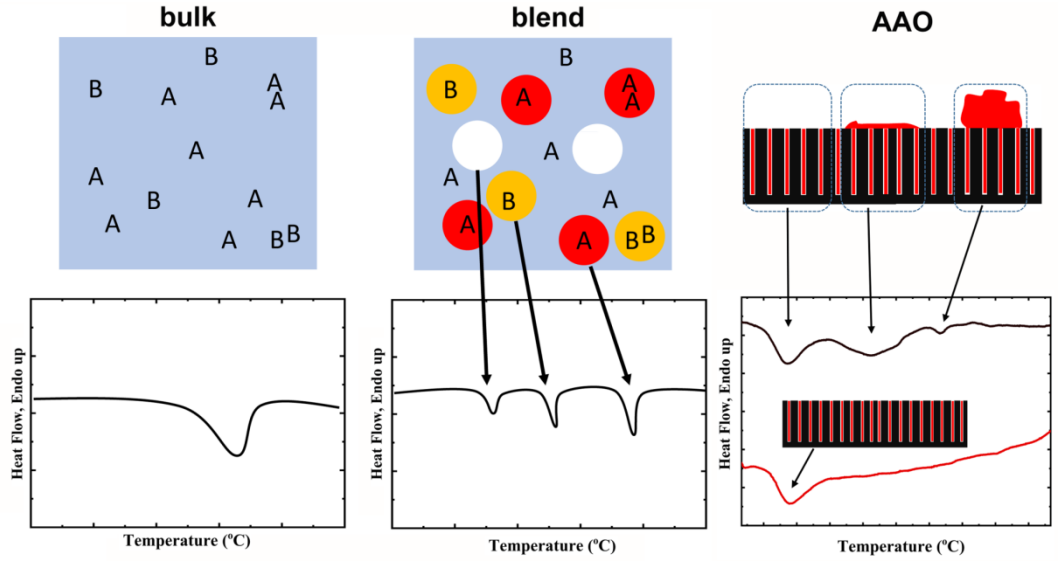

Figure 4. Schematic illustrating the origin of fractionated crystallization in blends and the effect of surface residue on the fractionated crystallization in AAO system. Adapted with permission from ref. [2], Copyright 2017 American Chemical Society.

2.2. Suppression of the Self-Nucleation Effect

Since the fractionated crystallization is decided by the relative numbers of nuclei and microdomains, in principle, introducing more nuclei will have an impact. Theoretically, the most effective way of enhancing nucleation is by self-nucleation.[44-46] Typically, the peak

crystallization temperature upon cooling from the melt, T_c, is independent of the temperature where the melt is cooled from (termed as T_s), if T_s is high enough to remove all the crystalline thermal history (in this case, the polymer is under *Domain I,* or full melting *Domain*, or isotropic melt *Domain*). By decreasing T_s, the crystallization will enter a *Domain* where the T_c shows an increase, while the T_m is essentially the same (*Domain II,* self-nucleation *Domain*). Further decreasing T_s will move the material into *Domain III*, the self-nucleation and annealing domain, where T_c increases, and there is an increase of T_m or a new melting peak characteristic of the annealed crystals. *Domain II* can be further divided into *Domain IIa*, where all the crystals are melted, and *Domain IIb*, where there are residual crystal fragments that can act as crystalline self-seeds. The typical concentration of self-nuclei at the lowest T_s of *Domain II* is in the order of $10^9 \sim 10^{12}$ cm^{-3},[44, 47] which is close to the density of AAO nanopores.

We studied the self-nucleation of PBS and PCL within AAO pores.[48] Figure 5 shows the temperature range of *Domain II* (and sub-domains) as a function of the density/diameter of AAO pores. Clearly, with decreasing the pore size, the width of *Domain II* decreases. *Domain IIa* disappears first, while *Domain IIb* vanishes within the smallest pores, indicating a total suppression of the self-nucleation effect. This suggests that the number of self-nuclei is still below the number of AAO pores in the high limit of AAO pore density. Interestingly, fractionated crystallization appears in self-nucleated infiltrated polymers. In *Domain II*, the pores can be divided by whether they contain self-nuclei or not. The pores that contain self-nuclei crystallize at a higher temperature, though the self-nuclei-free pores crystallize at a lower temperature as expected for homogeneous or surface nucleation mechanisms.

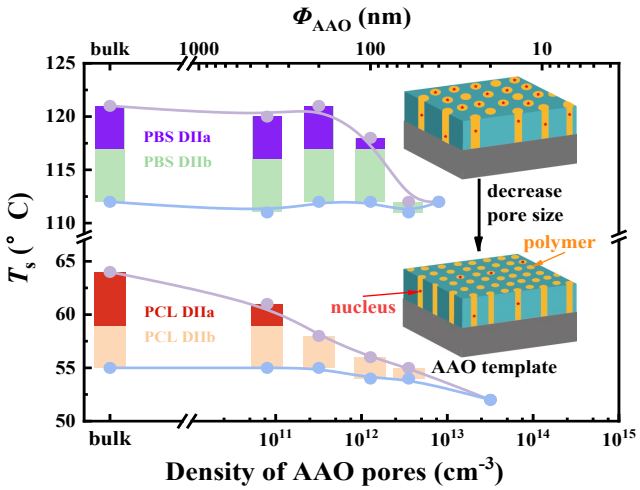

Figure 5. The effect of confinement on the self-nucleation *Domain* or *Domain II* (DII) for PBS and PCL. Reproduced with permission from ref. [48], Copyright 2021 American Chemical Society.

2.3. First Order Crystallization Kinetics

The overall crystallization kinetics of polymers (comprising both nucleation and growth) can be described by the Avrami equation:[49, 50]

$$1 - V_c(t) = e^{-k(t-t_0)^n}$$

where V_c is the volume fraction of crystals, and t is the crystallization time, t_0 the induction time, k the rate constant of overall crystallization, and n the Avrami index. The Avrami index, n, can be further expressed by the addition of two terms:[12, 51]

$$n = n_n + n_{gd}$$

where n_n is the nucleation term, and n_{gd} is related to the growth dimensionality. The n_n varies from 0 to 1, where 0 represents instantaneous nucleation and 1 corresponds to sporadic nucleation. Between these two extremes, n_n can be fractional values.

Figure 6 plots the n values of different polymers. A general observation of the crystallization kinetics of polymers within AAO pores is the reduction of n.[43] An approximate n value of 1 (i.e., in the range between 0.5 and 1.4), i.e., first-order kinetics, has been observed for infiltrated PEO and sPP.[29, 41, 52] The reason is that, in AAO pores, because of the small volume, the time needed for crystal grow is negligible as compared to the time needed for nucleation. Thus, the growth term, n_{gd}, becomes 0 independent of the geometry. Taking the sporadic nucleation term that is typical for homogeneous nucleation of confined polymers, the overall Avrami index becomes 1. When the nucleation becomes less sporadic, the n value can even become lower than 1 (see Figure 6).

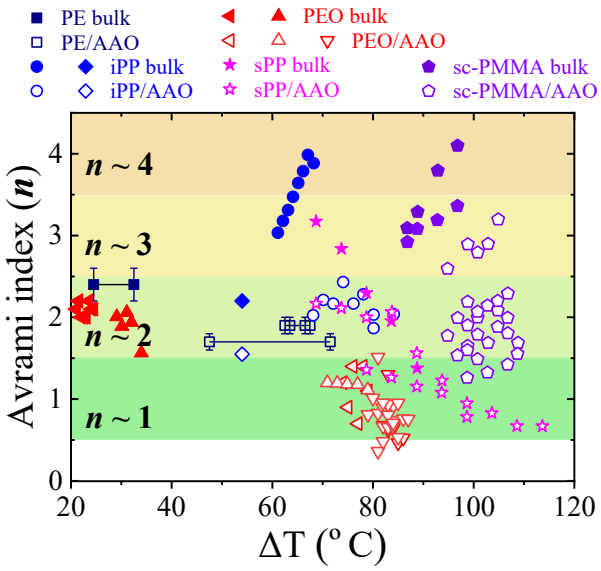

Figure 6. Avrami index of polymers plotted as a function of supercooling (ΔT). The bulk polymer is plotted as filled symbols and the infiltrated sample is plotted as hollow symbols. The data were taken from ref. [25] for PE, ref. [18] (blue circle) and [20] (blue diamond) for iPP, ref. [41] (red left triangle), [29] (red up triangle), and [52] (red down triangle) for PEO, ref. [33] (pink star) for sPP, ref. [53] for poly(methyl methacrylate) stereocomplex (sc-PMMA). The ΔT was calculated by the

difference of crystallization temperature and equilibrium melting temperature (T_m^o, values can be found in ref. [43]). For sc-PMMA, the highest melting temperature was used as T_m^o (510 K[54]).

2.4. Crystal Orientation

Controlling the orientation of crystallites provides an opportunity to tailor the physical properties of polymer materials for functional applications. Let's first focus on the thermodynamic effects. It is well known that polymer crystallizes into extended chain crystals when the molecular weight is below a critical value.[55] We chose a monodisperse PEO with a number average molecular weight of 2000 g/mol and a polydispersity index of 1.1. The PEO has a contour length of 12.6 nm, and only extended chain crystals are stable for this sample in bulk.[56] As shown in Figure 7, it was found that when the diameter of AAO is above the contour length of PEO, the chain in the crystal is perpendicular to the pore axis. On the other hand, when the diameter of AAO is 10 nm, the PEO chain aligns parallel to the AAO axis.[1] The results indicate that to maintain a thermodynamically stable conformation (extended chain crystal), the low molecular weight PEO adopts different orientations in the vicinity of a critical AAO diameter.

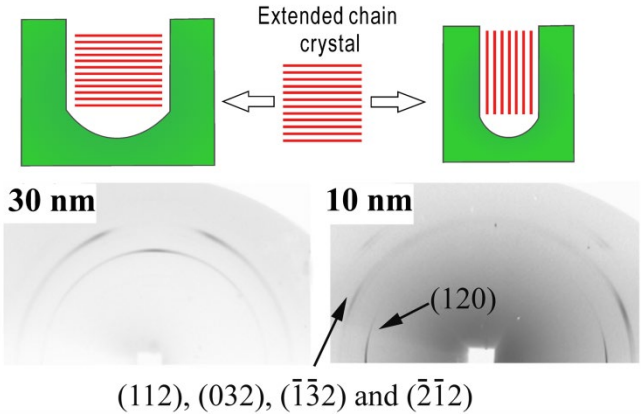

Figure 7. 2D WAXS patterns and orientation modes of monodisperse PEO within AAO tempaltes. Adapted with permission from ref. [1]. Copyright 2013 American Chemical Society.

The cylindrical geometry plays an essential role in selecting crystals that have the right orientation inside AAO pores. Steinhart et al.[23] proposed a "kinetic selection" model based on the study of PVDF/AAO. The core idea is shown in Figure 8A. The homogeneous nuclei inside the AAO pores are expected to be randomly oriented. If the growing direction of the crystals is parallel to the pore axis, the crystal will fill the space easily. However, if the growing direction is inclined to the pore axis, the crystal growth will be "blocked" by the AAO wall. Because polymer lamella grows perpendicular to the chain axis (*c*-axis), statistically, the final oriented structure of polymer crystals in separated AAO pores is one with the *c* axis perpendicular to the pore axis. On the other hand, if a surface reservoir is connected with the AAO, crystallization will start in the bulk and "grow into" the pore, resulting in the fastest growth direction (<020> for PVDF) parallel to the pore axis (Figure 8B). This indicates that the existence of a surface layer may alter the orientation of crystals inside the AAO pores.

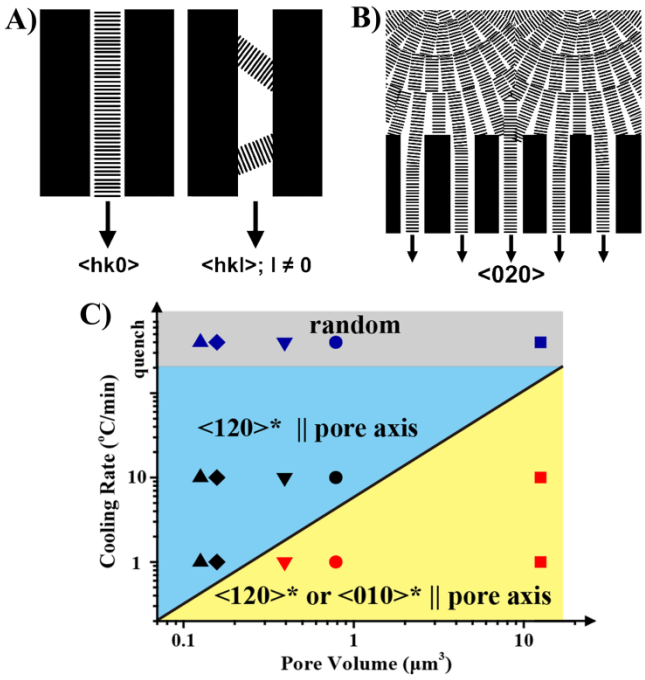

Figure 8. Schematic illustrating the kinetic selection of crystals: (A) without surface layer; (B) in connection with bulk reservoir. (C) Orientation diagram of PEO within AAO templates showing the effect of cooling rate and pore volume. Reproduced with permission from ref. [23] and [3]. Copyright 2006American Physical Society and Copyright 2018American Chemical Society.

One question of this model is whether the population of crystallites with <hk0> parallel to the pore axis is the same as that in the bulk. By noticing that the (020) reflection has a higher relative intensity in PVDF nanotubes within 400 nm AAO, Steinhart et al.[23] hypothesized that there could be several nuclei with different orientation coexisting within one pore, all of which are compatible with the kinetic selection rule (<hk0> parallel to the pore axis). In this case, crystal planes with a faster growth rate will dominate. Similar observations have also been reported in the crystallization of PEO blocks in the cylindrical phase of block copolymers, where the maximum growth direction ([120]) preferentially aligns along the pore axis.[57]

A survey of the literature indicates that PVDF is a unique example that shows all the (hk0) reflections with a similar intensity ratio as that of the bulk sample. Most frequently, one or two dominant crystal planes preferentially grow along the pore axis.[3] To elucidate the orientation of PEO within AAO pores and under different crystallization conditions, we measured the pole figure of PEO. The results lead to an orientation diagram. As shown in Figure 8C, the crystals in a quenched sample are isotropic, independent of the pore size. For relatively fast cooling in small pores (blue region), the (120) plane grows along the pore axis. However, mixed orientations are observed for larger pores under lower cooling (yellow region). This indicates that the crystal orientation of PEO in AAO is more complicated than the "kinetic selection" model. According to the single crystal growth studies,[58-60] the (010) plane becomes the fastest growth plane in PEO at higher crystallization temperature.

The orientation of polymer crystals within AAO was simulated by a 1D lattice model.[52, 61] The effect of growth rate and nucleation rate was considered. The results indicate three characteristic zones. When the nucleation rate is very high (corresponding to high supercooling), a large number of nuclei form simultaneously within a single AAO pore via homogeneous nucleation. The dimension of crystal growth is very limited. As the nuclei are isotropic, the overall orientation of polymer crystals is isotropic as well. In another limit, when the nucleation rate is very low, and the growth rate is high, statistically, any nucleus that matches the selection rule (Figure 8A) is able to grow and fill the pore rapidly before another nucleus can form. In the middle zone, where the nucleation rate and growth rate are both intermediate, several nuclei will form in a pore, and the growth rates of the various planes determine the populations of crystal orientations.

2.5. Surface/Interface Effect

We have so far only considered the size effect and geometrical effect on polymer crystallization inside AAO. Polymer chains are in contact with the inorganic AAO wall. The interactions should influence the crystallization of polymers on nucleation and/or chain mobility. However, the studies on the impact of the interface on the crystallization behavior of polymers within AAO are rare, and it is often difficult to disentangle the impact of interface and the impact of lack of nucleation sites.[62-64] Surface nucleation has been argued in infiltrated PE[26] and PBS[32], based on the idea that homogeneous nucleation only occurs at a temperature close to T_g, and the T_cs of the two polymers are well above their T_gs.

An unusual acceleration of cold crystallization was observed in poly(L-lactic acid) (PLLA).[65] As shown in Figure 9A, the crystallization rate increases significantly with decreasing pore size.

This indicates that there must be a different mechanism for crystal nucleation in PLLA. To reveal the possible interactions, an amorphous PDLLA was used instead of PLLA to eliminate the influence of crystallization on the dielectric signal. Two T_gs were observed in the heating run of quenched PDLLA, as shown in Figure 9B, one of which is located at a similar temperature as the bulk sample, while a low-temperature peak appears. This indicates that there is a fraction of chains with higher mobility. Indeed, the segmental relaxation time of the infiltrated samples deviates from the bulk sample at the lower temperature side, where the segmental relaxation time decreases with decreasing pore diameter. According to the classical nucleation theory,[66] the nucleation rate can be expressed as:

$$I = I_0 \exp\left(-\frac{\Delta G^* + \Delta E}{kT}\right)$$

where ΔG^* is the free energy barrier of forming a critical nucleus, and ΔE is the activation energy of diffusion of segments across the phase boundary. The accelerated nucleation of PLLA within AAO is most probably induced by a reduced diffusion barrier ΔE. This is physically similar to the case of amorphous thin films, where a free surface layer exhibits faster dynamics, i.e., a lower T_g.[67] A high mobility interfacial layer was also observed in PMMA/AAO system.[68, 69] Further experiments showed that the mobility of the interfacial layer decreased during annealing just above T_g, indicating that the interfacial layer is in a non-equilibrium state. As a result, the nucleation of PLLA decreases during annealing.

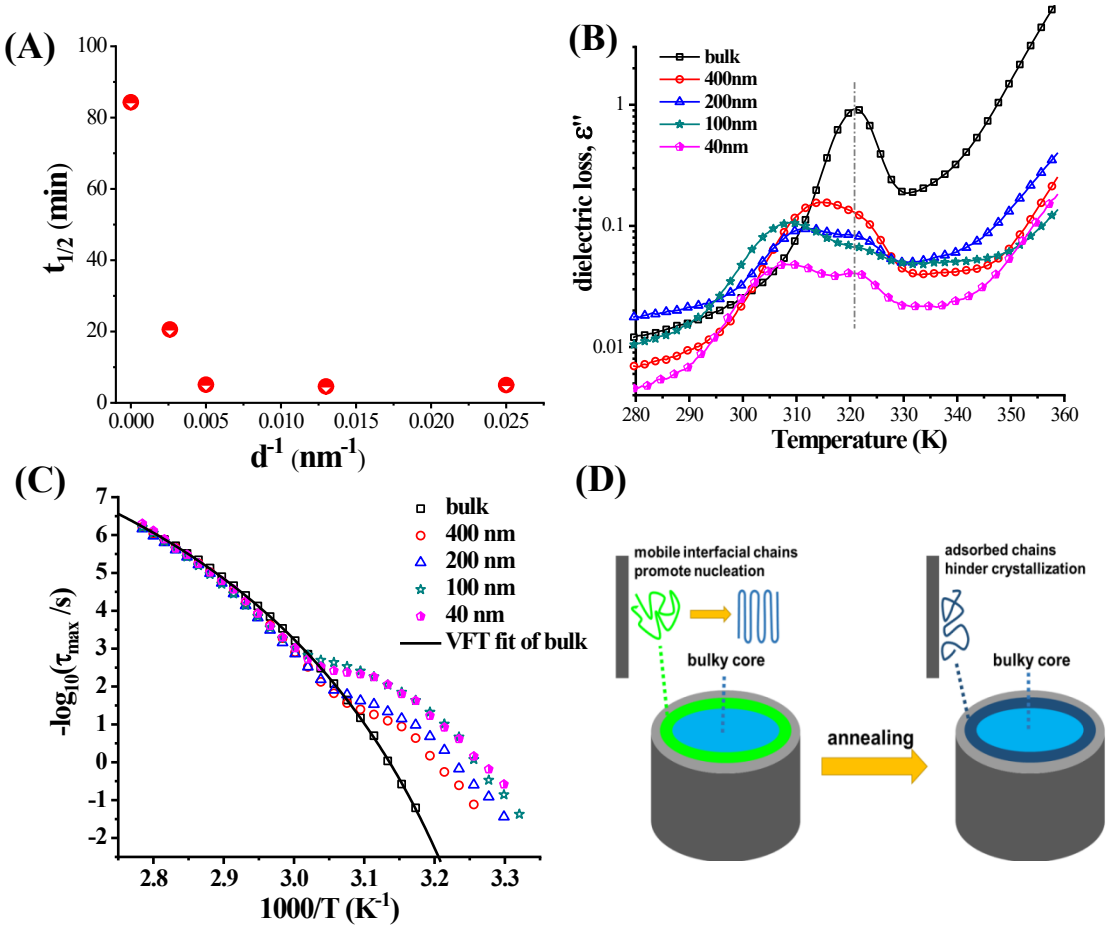

Figure 9. (A) Crystallization half time of PLLA at 75 °C as a function of the inverse diameter of AAO pores; (B) dielectric loss of melt quenched PDLLA during heating; (C) Arrhenius plot of PDLLA within AAO pores measured during heating of quenched samples; (D) schematic illustrating the existence of interfacial layer with segmental mobility depending on the thermal history. Reproduced with permission from ref. [65] and [4]. Copyright 2015 and 2019American Chemical Society.

Another example of the interfacial effect on crystalline polymers is the polymorphic phase transition in polybutene-1 (PB-1).[37] Under melt crystallization conditions, PB-1 crystallizes into a metastable phase (Form II), characterized by a 11_3 helical conformation in a tetragonal unit cell.

During annealing, Form II transforms instantaneously into the stable Form I phase. As shown in WAXS results (Figure 10A), it is obvious that the intensity of Form II reflections decreases with annealing at room temperature. The reflections of Form I gradually appear as a function of time. The change of the Form I fraction of bulk and infiltrated PB-1 is plotted in Figure 10B. Two features are visible: (a) the rate change is different among different samples; (b) the saturation fraction of Form I, $X_{I\infty}$, decreases with confinement. Surprisingly, the PB-1 infiltrated within 30 nm AAO does not show any transition. To account for the reduced transition degree, the $X_{I\infty}$ can be fitted by a simple formula:

$$X_{I\infty} = \left(1 - \frac{2l}{d}\right)^2$$

This formula agrees with a two-layer model with a 12 nm interfacial layer that does not transform to Form I.

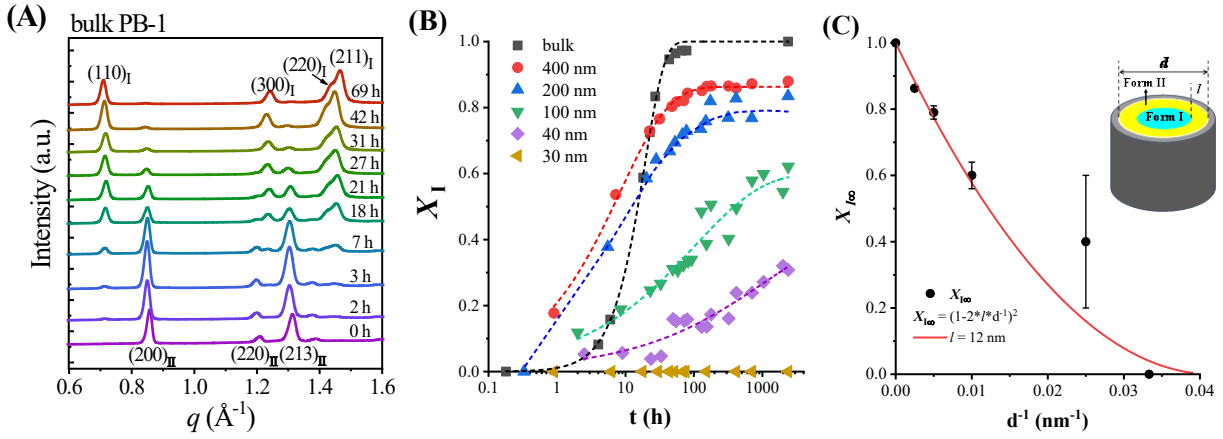

Figure 10. (A) WAXS curves of PB-1 during annealing at room temperature indicating the transition of Form II to Form I. (B) The degree of transition X_I as a function of annealing time. (C) The maximum transition degree ($X_{I\infty}$) as a function of the inverse pore diameter. Reproduced with permission from ref. [37]. Copyright 2020 American Chemical Society.

The crystallization or crystal transition rate of polymer is determined by factors that originate from finite size and interfacial effects. Prediction of the crystallization rates has been challenging. For polymers under 1D confinement (thin films), an analytical model was proposed to estimate the time scale for crystallization, by assuming the crystallization rate can be expressed by a product of the probabilities involving nucleation and chain diffusion.[70]

2.6. From Homopolymers to Copolymers

Confined crystallization of polymers has been extended to more complicated systems such as block copolymers and random copolymers. In strongly segregated PE-*b*-PS diblock copolymers, the PE crystalline phase experienced double confinement.[26] The T_c shifts to lower temperatures. All the copolymers show a core-shell morphology, where PE block forms the shell in contact with the AAO wall.[71] Similar to the infiltrated homopolymer, the nucleation mechanism of the PE component of PE-*b*-PS is assigned to surface nucleation. In crystalline-crystalline PCL-*b*-PEO diblock copolymer, the crystallization of PEO was suppressed by the double confinement of AAO and crystalline PCL.[40]

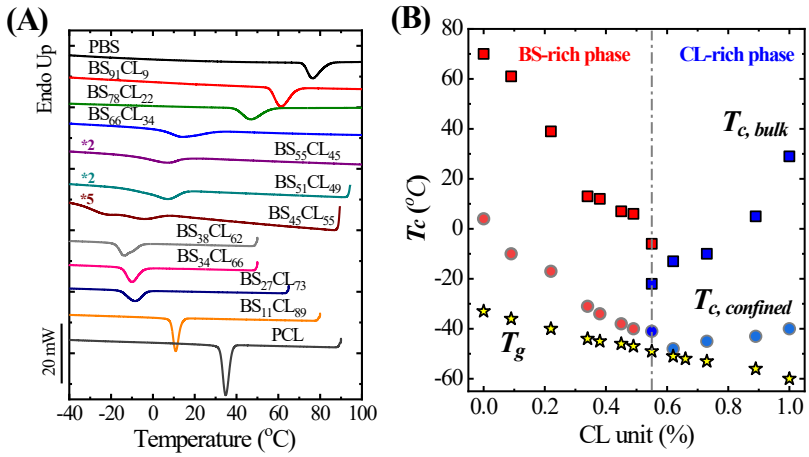

Figure 11. (A) DSC cooling curves of PBS-ran-PCL with different compositions. (B) Summary of the T_c of the bulk and infiltrated copolymers together with the T_g. Reproduced with permission from ref. [72] and [73]. Copyright 2018 and 2020 American Chemical Society.

Random copolymers show interesting comonomer inclusion or comonomer exclusion behavior depending on the miscibility of comonomers in the crystalline phase. Figure 11A shows the DSC cooling curves of random copolymers of butylene succinate and caprolactone (PBS-*ran*-PCL, BS_xCL_{100-x}).[72] For most of the copolymers, only one crystallization peak was observed. The crystallization and melting temperatures decrease with comonomer contents and go through a pseudo-eutectic point that is characteristic of isodimorphic random copolymers. In these isodimorphic copolymers, the PBS-rich compositions exhibit a similar crystalline structure as PBS homopolymer but with small inclusions of CL comonomer units, and conversely, the PCL-rich compositions exhibit a similar crystalline structure as PCL homopolymer but with small inclusions of BS comonomer units.[72, 74] For $BS_{45}CL_{55}$, two crystallization peaks were observed (at the pseudoeutectic point), indicating two crystalline phases, one PBS-rich and another PCL-rich. A series of isodimorphic PBS-*ran*-PCL polymers were infiltrated into AAO templates with a diameter of 100 nm.[73] Figure 11B summarizes the crystallization temperatures of the bulk and infiltrated PBS-*ran*-PCL. Only one T_g was observed (as the amorphous phases are miscible in the random copolymers), which changed linearly with composition. After infiltration, a very large reduction in crystallization temperature can be observed for all the copolymers, which is in accordance to that observed in homopolymers. Interestingly, the isodimorphic behavior of the copolyesters is maintained for the infiltrated copolymers.

3. CONCLUSIONS AND OUTLOOK

In summary, AAO nanopores provide an ideal 1D cylindrical environment to explore the basic mechanism of confined crystallization of polymers. We have shown that infiltrated polymers crystallize distinctly different from the bulk. A message from the experimental point of view is the importance of surface residue, which is the origin of fractionated crystallization and also influences the orientation of the crystals. Because the number of heterogeneities in a bulk polymer is several orders of magnitude lower than the number of nanopores within theAAO, the nucleation mechanism changes from heterogeneous nucleation to homogeneous/surface nucleation. By introducing self-nuclei, the nuclei density can be comparable to the pore density of AAO. The self-nucleation effect is completely suppressed in AAO pores with the lowest diameter (below 60 nm). Fractionated crystallization "reappears" in self-nucleated polymer inside AAO due to the co-existence of self-nuclei and surface or homogeneous nuclei. Polymer crystals inside AAO exhibit anisotropic structures, which are determined by thermodynamic stability and kinetic selection rules, including chain conformation, nucleation rate, and growth rates of different crystal planes. The interface between polymer and AAO has an impact on the nucleation of PLLA and polymorphic transition in PB-1. The confinement study in AAO nanopores was extended to block and random copolymers.

There are open questions that remain unsolved. First, the usual diameter of AAO nanopores (ranging between 400 and 20 nm) is above the radius of gyration, critical nucleus size, and lamellar thickness of typical polymers. Therefore, the confinement effect does not reach the smallest length scale of polymeric crystals. Developing templates with smaller pores will be interesting to push the limit to even smaller dimensions. Secondly, there is still a lack of general understanding of how the interfacial interaction affects the nucleation of polymers. The

development of surface modification techniques and the study of the impact of specific interactions may provide crucial evidence of the factors affecting surface nucleation.

AUTHOR INFORMATION

Corresponding Authors

Alejandro J. Müller

POLYMAT and Department of Polymers and Advanced Materials: Physics, Chemistry and Technology, Faculty of Chemistry, University of the Basque Country UPV/EHU, Paseo Manuel de Lardizabal, 3, 20018 Donostia-San Sebastián, Spain; IKERBASQUE, Basque Foundation for Science, Bilbao, 48009, Spain; orcid.org/0000-0001-7009-7715

Email: alejandrojesus.muller@ehu.es

Dujin Wang

Beijing National Laboratory for Molecular Sciences, Institute of Chemistry, Chinese Academy of Sciences, Beijing 100190, China; University of Chinese Academy of Sciences, Beijing 100049, China; orcid.org/0000-0002-2063-0873

Email: djwang@iccas.ac.cn

Author

Guoming Liu

Beijing National Laboratory for Molecular Sciences, Institute of Chemistry, Chinese Academy of Sciences, Beijing 100190, China; University of Chinese Academy of Sciences, Beijing 100049, China; orcid.org/0000-0003-2808-2661

Email: gmliu@iccas.ac.cn

Author Contributions

The manuscript was written through contributions of all authors. All authors have given approval to the final version of the manuscript.

Notes

The authors declare no competing financial interest.

Biographies

Guoming Liu is a Professor of ICCAS in Beijing. He received his B.Sc. in 2006 from Sichuan University and Ph.D. in 2011 from ICCAS under the supervision of Prof. Dujin Wang. Since then, he has been working at ICCAS, first as an Assistant Professor and then as an Associate Professor since 2014. From 2016 to 2018, he was a postdoctoral researcher at Cavendish Laboratory, University of Cambridge, as a Newton International Fellow of the Royal Society. In 2019, he received the Outstanding Youth Science Foundation Grant of NSFC. Since 2019, he was appointed Professor of ICCAS. His research interests include structure-property relationships of polymers, polymer crystallization and relaxation in confined space, and polymer structure characterization by X-ray and neutron scattering.

Alejandro J. Müller is a Materials Engineer (Simón Bolívar University, Caracas, Venezuela), with an M.Sc. in Chemistry (Venezuelan Institute for Scientific Research, IVIC, Caracas, Venezuela) and a Ph.D. in Physics (Bristol University, U.K.; advisors: Andrew Keller and Jeff Odell). He worked for nearly 30 years as a professor at the Materials Science Department of Simón Bolívar University in Caracas, Venezuela, where he founded and coordinated a very productive research group in Polymer Science. He is a Corresponding Member of the "Academia Nacional de la Ingenierıa y del Habitat de Venezuela (ANIH)" or National Academy of Engineering and Habitat from Venezuela. He won several awards in Venezuela, including the Lorenzo Mendoza Fleury, Polar Prize for basic science (in chemistry). In 2011, he received the international "Paul J. Flory Polymer Research Prize" for his contributions to Confined Crystallization research. He was recently elected a corresponding member of the Latin American Academy of Sciences (2021). Since September 2013, he holds an IKERBASQUE (Basque Foundation for Science) Research Chair at POLYMAT and Department of Polymers and Advanced Materials: Physics, Chemistry and Technology, Faculty of Chemistry, University of the Basque Country UPV/EHU in Donostia-San Sebastián, Spain, where he leads the Advanced Multiphasic Polymers Group. He is an Editor for Polymer (Elsevier) in the joint areas of Polymer Physics and Physical Chemistry. His fields of interest include structure, morphology, nucleation, crystallization, crystallization kinetics, rheology, and properties of multiphasic and confined polymeric materials (in particular, block copolymers, random copolymers, nanocomposites, hybrids, and polymer blends).

Dujin Wang is a professor of ICCAS in Beijing. He received his Ph.D. in 1995 from Peking University under the supervision of Prof. Jinguang Wu. After two years of postdoctoral research at ICCAS with Prof. Duanfu Xu, he joined the institute as a faculty member in 1997. In 2000, he was appointed to a professorship at ICCAS. In 2009, he received a grant from the National Natural Science Foundation of China for Distinguished Young Scholars. He was the director of CAS Key Laboratory of Engineering Plastics (2004-2014) and the deputy director of ICCAS

(2008-2020). He is currently the Executive Deputy Director of the Polymer Division of the Chinese Chemical Society, Associate Editor for Chinese Journal of Polymer Science, and Acta Polymerica Sinica. He is a Fellow of the American Chemical Society and the Royal Society of Chemistry, and an Advanced Member of the Chinese Chemical Society. His research interests include polymer morphology and processing, crystallization and orientation.

ACKNOWLEDGMENTS

This work was supported by the National Key R&D Program of China (2017YFE0117800) and the National Natural Science Foundation of China (21873109, 51820105005, 21922308). We would also like to acknowledge the financial support from the BIODEST project, this project has received funding from the European Union's Horizon 2020 research and innovation programme under the Marie Skłodowska-Curie grant agreement No 778092. A.J.M. acknowledges funding from MINECO, MAT2017-83014-C2-1-P, and from the Basque Government through grant IT1309-19. G.L. is grateful to the Youth Innovation Promotion Association of the Chinese Academy of Sciences (Y201908).

REFERENCES

1. Guan, Y.; Liu, G.; Gao, P.; Li, L.; Ding, G.; Wang, D. Manipulating Crystal Orientation of Poly(ethylene oxide) by Nanopores. *ACS Macro Letters* **2013,** 2 (3), 181-184 DOI: 10.1021/mz300592v.
2. Shi, G.; Liu, G.; Su, C.; Chen, H.; Chen, Y.; Su, Y.; Müller, A. J.; Wang, D. Reexamining the Crystallization of Poly(ε-caprolactone) and Isotactic Polypropylene under Hard Confinement: Nucleation and Orientation. *Macromolecules* **2017,** 50 (22), 9015-9023 DOI: 10.1021/acs.macromol.7b02284.
3. Su, C.; Shi, G.; Li, X.; Zhang, X.; Müller, A. J.; Wang, D.; Liu, G. Uniaxial and Mixed Orientations of Poly(ethylene oxide) in Nanoporous Alumina Studied by X-ray Pole Figure Analysis. *Macromolecules* **2018,** 51 (23), 9484-9493 DOI: 10.1021/acs.macromol.8b01801.
4. Shi, G.; Guan, Y.; Liu, G.; Müller, A. J.; Wang, D. Segmental Dynamics Govern the Cold Crystallization of Poly(lactic acid) in Nanoporous Alumina. *Macromolecules* **2019,** 52 (18), 6904-6912 DOI: 10.1021/acs.macromol.9b00542.
5. Lodge, T. P. Celebrating 50 Years of Macromolecules. *Macromolecules* **2017,** 50 (24), 9525-9527 DOI: 10.1021/acs.macromol.7b02507.
6. Lotz, B.; Miyoshi, T.; Cheng, S. Z. D. 50th Anniversary Perspective: Polymer Crystals and Crystallization: Personal Journeys in a Challenging Research Field. *Macromolecules* **2017,** 50 (16), 5995-6025 DOI: 10.1021/acs.macromol.7b00907.
7. Keller, A.; Cheng, S. Z. D. The role of metastability in polymer phase transitions. *Polymer* **1998,** 39 (19), 4461-4487 DOI: http://dx.doi.org/10.1016/S0032-3861(97)10320-2.
8. Hoffman, J. D.; Miller, R. L. Kinetics of crystallization from the melt and chain folding in polyethylene fractions revisited: Theory and experiment. *Polymer* **1997,** 38 (13), 3151-3212.
9. Hamley, I. W., *the Physics of Block Copolymers*. Oxford University Press: London, 1998.
10. Hamley, I. W., *Developments in Block Copolymer Science and Technology*. John Wiley & Sons Ltd: Chichester, 2004.
11. Müller, A. J.; Balsamo, V.; Arnal, M. L.; Jakob, T.; Schmalz, H.; Abetz, V. Homogeneous Nucleation and Fractionated Crystallization in Block Copolymers†. *Macromolecules* **2002,** 35 (8), 3048-3058 DOI: 10.1021/ma012026w.

12. Müller, A. J.; Balsamo, V.; Arnal, M. L., Nucleation and Crystallization in Diblock and Triblock Copolymers. In *Block Copolymers II*, Abetz, V., Ed. Springer Berlin Heidelberg: Berlin, Heidelberg, 2005; pp 1-63.
13. Michell, R. M.; Müller, A. J. Confined crystallization of polymeric materials. *Progress in Polymer Science* **2016,** 54, 183-213 DOI: http://dx.doi.org/10.1016/j.progpolymsci.2015.10.007.
14. Masuda, H.; Fukuda, K. Ordered metal nanohole arrays made by a two-step replication of honeycomb structures of anodic alumina. *Science* **1995,** 268 (5216), 1466-1468.
15. Masuda, H.; Satoh, M. Fabrication of Gold Nanodot Array Using Anodic Porous Alumina as an Evaporation Mask. *Japanese Journal of Applied Physics* **1996,** 35 (Part 2, No. 1B), L126-L129 DOI: 10.1143/jjap.35.l126.
16. Steinhart, M.; Wendorff, J. H.; Greiner, A.; Wehrspohn, R. B.; Nielsch, K.; Schilling, J.; Choi, J.; Gösele, U. Polymer Nanotubes by Wetting of Ordered Porous Templates. *Science* **2002,** 296 (5575), 1997 DOI: 10.1126/science.1071210.
17. Lee, W.; Park, S.-J. Porous Anodic Aluminum Oxide: Anodization and Templated Synthesis of Functional Nanostructures. *Chemical Reviews* **2014,** 114 (15), 7487-7556 DOI: 10.1021/cr500002z.
18. Duran, H.; Steinhart, M.; Butt, H.-J.; Floudas, G. From Heterogeneous to Homogeneous Nucleation of Isotactic Poly(propylene) Confined to Nanoporous Alumina. *Nano Letters* **2011,** 11 (4), 1671-1675 DOI: 10.1021/nl200153c.
19. Liu, G.; Shi, G.; Wang, D. Research Progress on Polymer Crystallization Confined within Nano-porous AAO Templates. *Acta Polymerica Sinica* **2020,** 51 (5), 501-516 DOI: -10.11777/j.issn1000-3304.2020.20003.
20. Reid, D. K.; Ehlinger, B. A.; Shao, L.; Lutkenhaus, J. L. Crystallization and orientation of isotactic poly(propylene) in cylindrical nanopores. *Journal of Polymer Science Part B: Polymer Physics* **2014,** 52 (21), 1412-1419 DOI: 10.1002/polb.23577.
21. Suzuki, Y.; Duran, H.; Akram, W.; Steinhart, M.; Floudas, G.; Butt, H. J. Multiple nucleation events and local dynamics of poly(epsilon-caprolactone) (PCL) confined to nanoporous alumina. *Soft Matter* **2013,** 9 (38), 9189-9198 DOI: 10.1039/c3sm50907a.
22. Sanz, B.; Blaszczyk-Lezak, I.; Mijangos, C.; Palacios, J. K.; Müller, A. J. New Double-Infiltration Methodology to Prepare PCL–PS Core–Shell Nanocylinders Inside Anodic Aluminum Oxide Templates. *Langmuir* **2016,** 32 (31), 7860-7865 DOI: 10.1021/acs.langmuir.6b01258.
23. Steinhart, M.; Goring, P.; Dernaika, H.; Prabhukaran, M.; Gosele, U.; Hempel, E.; Thurn-Albrecht, T. Coherent kinetic control over crystal orientation in macroscopic ensembles of polymer nanorods and nanotubes. *Physical Review Letters* **2006,** 97 (2), 027801 DOI: 10.1103/PhysRevLett.97.027801.
24. Dai, X.; Niu, J.; Ren, Z.; Sun, X.; Yan, S. Effects of Nanoporous Anodic Alumina Oxide on the Crystallization and Melting Behavior of Poly(vinylidene fluoride). *The Journal of Physical Chemistry B* **2016,** 120 (4), 843-850 DOI: 10.1021/acs.jpcb.5b11178.
25. Woo, E.; Huh, J.; Jeong, Y. G.; Shin, K. From Homogeneous to Heterogeneous Nucleation of Chain Molecules under Nanoscopic Cylindrical Confinement. *Physical Review Letters* **2007,** 98 (13), 136103.
26. Michell, R. M.; Lorenzo, A. T.; Müller, A. J.; Lin, M.-C.; Chen, H.-L.; Blaszczyk-Lezak, I.; Martín, J.; Mijangos, C. The Crystallization of Confined Polymers and Block Copolymers Infiltrated Within Alumina Nanotube Templates. *Macromolecules* **2012,** (45), 1517-1528 DOI: 10.1021/ma202327f.

27. Wu, H.; Wang, W.; Yang, H.; Su, Z. Crystallization and Orientation of Syndiotactic Polystyrene in Nanorods. *Macromolecules* **2007,** 40, 4244-4249.
28. Liu, C.-L.; Chen, H.-L. Crystal orientation of PEO confined within the nanorod templated by AAO nanochannels. *Soft Matter* **2018**, DOI: 10.1039/C8SM00795K.
29. Maiz, J.; Martin, J.; Mijangos, C. Confinement Effects on the Crystallization of Poly(ethylene oxide) Nanotubes. *Langmuir* **2012,** 28 (33), 12296-12303 DOI: 10.1021/la302675k.
30. Suzuki, Y.; Duran, H.; Steinhart, M.; Butt, H.-J.; Floudas, G. Homogeneous crystallization and local dynamics of poly(ethylene oxide) (PEO) confined to nanoporous alumina. *Soft Matter* **2013,** 9 (9), 2621-2628 DOI: 10.1039/c2sm27618f.
31. Mi, C.; Zhou, J.; Ren, Z.; Li, H.; Sun, X.; Yan, S. The phase transition behavior of poly(butylene adipate) in the nanoporous anodic alumina oxide. *Polymer Chemistry* **2016,** 7 (2), 410-417 DOI: 10.1039/C5PY01532D.
32. Safari, M.; Maiz, J.; Shi, G.; Juanes, D.; Liu, G.; Wang, D.; Mijangos, C.; Alegría, Á.; Müller, A. J. How Confinement Affects the Nucleation, Crystallization, and Dielectric Relaxation of Poly(butylene succinate) and Poly(butylene adipate) Infiltrated within Nanoporous Alumina Templates. *Langmuir* **2019,** 35 (47), 15168-15179 DOI: 10.1021/acs.langmuir.9b02215.
33. Li, L.; Liu, J.; Qin, L.; Zhang, C.; Sha, Y.; Jiang, J.; Wang, X.; Chen, W.; Xue, G.; Zhou, D. Crystallization kinetics of syndiotactic polypropylene confined in nanoporous alumina. *Polymer* **2017,** 110 (Supplement C), 273-283 DOI: https://doi.org/10.1016/j.polymer.2016.12.081.
34. Wu, H.; Higaki, Y.; Nojima, S.; Takahara, A. Orientation and crystallization of regioregular poly(3-dodecylthiophene) in alumina nanopores. *Soft Matter* **2017**, DOI: 10.1039/C7SM00859G.
35. Dai, X.; Li, H.; Ren, Z.; Russell, T. P.; Yan, S.; Sun, X. Confinement Effects on the Crystallization of Poly(3-hydroxybutyrate). *Macromolecules* **2018,** 51 (15), 5732-5741 DOI: 10.1021/acs.macromol.8b01083.
36. Yu, S.; Lai, Z.; Jinnai, H.; Zeng, X.; Ageishi, M.; Lotz, B.; Cheng, S. Z. D.; Zheng, N.; Zhang, S.; Feng, X.; Cao, Y. Adding Symmetry: Cylindrically Confined Crystallization of Nylon-6. *Macromolecules* **2019**, DOI: 10.1021/acs.macromol.8b02672.
37. Shi, G.; Wang, Z.; Wang, M.; Liu, G.; Cavallo, D.; Müller, A. J.; Wang, D. Crystallization, Orientation, and Solid–Solid Crystal Transition of Polybutene-1 Confined within Nanoporous Alumina. *Macromolecules* **2020,** 53 (15), 6510-6518 DOI: 10.1021/acs.macromol.0c01384.
38. Wunderlich, B., CHAPTER V - The Nucleation Step. In *Macromolecular Physics*, Wunderlich, B., Ed. Academic Press: 1976; pp 1-114.
39. Wu, H.; Wang, W.; Huang, Y.; Wang, C.; Su, Z. Polymorphic Behavior of Syndiotactic Polystyrene Crystallized in Cylindrical Nanopores. *Macromolecules* **2008,** 41 (20), 7755-7758 DOI: 10.1021/ma801498b.
40. Suzuki, Y.; Duran, H.; Steinhart, M.; Butt, H.-J.; Floudas, G. Suppression of Poly(ethylene oxide) Crystallization in Diblock Copolymers of Poly(ethylene oxide)-b-poly(epsilon-caprolactone) Confined to Nanoporous Alumina. *Macromolecules* **2014,** 47 (5), 1793-1800 DOI: 10.1021/ma4026477.

41. Michell, R. M.; Blaszczyk-Lezak, I.; Mijangos, C.; Müller, A. J. Confinement effects on polymer crystallization: From droplets to alumina nanopores. *Polymer* **2013,** 54 (16), 4059-4077 DOI: https://doi.org/10.1016/j.polymer.2013.05.029.
42. Groeninckx, G.; Harrats, C.; Vanneste, M.; Everaert, V., Crystallization, Micro- and Nano-structure, and Melting Behavior of Polymer Blends. In *Polymer Blends Handbook*, Utracki, L. A., Wilkie, C. A., Eds. Springer Netherlands: Dordrecht, 2014; pp 291-446.
43. Sangroniz, L.; Wang, B.; Su, Y.; Liu, G.; Cavallo, D.; Wang, D.; Müller, A. J. Fractionated crystallization in semicrystalline polymers. *Progress in Polymer Science* **2021,** 115, 101376 DOI: https://doi.org/10.1016/j.progpolymsci.2021.101376.
44. Fillon, B.; Wittmann, J. C.; Lotz, B.; Thierry, A. Self-nucleation and recrystallization of isotactic polypropylene (α phase) investigated by differential scanning calorimetry. *Journal of Polymer Science Part B: Polymer Physics* **1993,** 31 (10), 1383-1393 DOI: doi:10.1002/polb.1993.090311013.
45. Fillon, B.; Lotz, B.; Thierry, A.; Wittmann, J. C. Self-nucleation and enhanced nucleation of polymers. Definition of a convenient calorimetric "efficiency scale" and evaluation of nucleating additives in isotactic polypropylene (α phase). *Journal of Polymer Science Part B: Polymer Physics* **1993,** 31 (10), 1395-1405 DOI: https://doi.org/10.1002/polb.1993.090311014.
46. Michell, R. M.; Mugica, A.; Zubitur, M.; Müller, A. J., Self-Nucleation of Crystalline Phases Within Homopolymers, Polymer Blends, Copolymers, and Nanocomposites. In *Polymer Crystallization I: From Chain Microstructure to Processing*, Auriemma, F., Alfonso, G. C., de Rosa, C., Eds. Springer International Publishing: Cham, 2017; pp 215-256.
47. Sangroniz, L.; Cavallo, D.; Müller, A. J. Self-Nucleation Effects on Polymer Crystallization. *Macromolecules* **2020,** 53 (12), 4581-4604 DOI: 10.1021/acs.macromol.0c00223.
48. Wang, M.; Li, J.; Shi, G.; Liu, G.; Müller, A. J.; Wang, D. Suppression of the Self-Nucleation Effect of Semicrystalline Polymers by Confinement. *Macromolecules* **2021**, DOI: 10.1021/acs.macromol.1c00485.
49. Avrami, M. Granulation, Phase Change, and Microstructure Kinetics of Phase Change. III. *The Journal of Chemical Physics* **1941,** 9 (2), 177-184 DOI: 10.1063/1.1750872.
50. Lorenzo, A. T.; Arnal, M. L.; Albuerne, J.; Müller, A. J. DSC isothermal polymer crystallization kinetics measurements and the use of the Avrami equation to fit the data: Guidelines to avoid common problems. *Polymer Testing* **2007,** 26 (2), 222-231 DOI: https://doi.org/10.1016/j.polymertesting.2006.10.005.
51. Balsamo, V.; Urdaneta, N.; Pérez, L.; Carrizales, P.; Abetz, V.; Müller, A. J. Effect of the polyethylene confinement and topology on its crystallisation within semicrystalline ABC triblock copolymers. *European Polymer Journal* **2004,** 40 (6), 1033-1049 DOI: https://doi.org/10.1016/j.eurpolymj.2004.01.009.
52. Su, C.; Chen, Y.; Shi, G.; Li, T.; Liu, G.; Müller, A. J.; Wang, D. Crystallization Kinetics of Poly(ethylene oxide) under Confinement in Nanoporous Alumina Studied by in Situ X-ray Scattering and Simulation. *Langmuir* **2019,** 35 (36), 11799-11808 DOI: 10.1021/acs.langmuir.9b01968.
53. Lin, Y.-L.; Tsai, S.-Y.; He, H.-C.; Lee, L.-R.; Ho, J.-H.; Wang, C.-L.; Chen, J.-T. Crystallization of Poly(methyl methacrylate) Stereocomplexes under Cylindrical Nanoconfinement. *Macromolecules* **2021,** 54 (4), 2001-2010 DOI: 10.1021/acs.macromol.0c02585.

54. Lemieux, E. J.; Prud'homme, R. E. Crystallization behaviour of stereocomplexed poly(methyl methacrylates): influence of thermal history. *Polymer* **1998,** 39 (22), 5453-5460 DOI: https://doi.org/10.1016/S0032-3861(97)10163-X.
55. Strobl, G., *The physics of polymers*. 2nd ed.; Springer: New York, 2006.
56. Song, K.; Krimm, S. Raman longitudinal acoustic mode (LAM) studies of folded-chain morphology in poly(ethylene oxide) (PEO). 3. Chain folding in PEO as a function of molecular weight. *Macromolecules* **1990,** 23 (7), 1946-1957 DOI: 10.1021/ma00209a012.
57. Huang, P.; Zhu, L.; Cheng, S. Z. D.; Ge, Q.; Quirk, R. P.; Thomas, E. L.; Lotz, B.; Hsiao, B. S.; Liu, L.; Yeh, F. Crystal Orientation Changes in Two-Dimensionally Confined Nanocylinders in a Poly(ethylene oxide)-b-polystyrene/Polystyrene Blend. *Macromolecules* **2001,** 34 (19), 6649-6657 DOI: 10.1021/ma010671x.
58. Marentette, J. M.; Brown, G. R. The (010)–(120) crystal growth face transformation in poly(ethylene oxide) spherulites. *Polymer* **1998,** 39 (6), 1405-1414 DOI: https://doi.org/10.1016/S0032-3861(97)00554-5.
59. Zhai, X.; Wang, W.; Zhang, G.; He, B. Crystal Pattern Formation and Transitions of PEO Monolayers on Solid Substrates from Nonequilibrium to near Equilibrium. *Macromolecules* **2006,** 39 (1), 324-329 DOI: 10.1021/ma051624y.
60. Zhang, G.; Cao, Y.; Jin, L.; Zheng, P.; Van Horn, R. M.; Lotz, B.; Cheng, S. Z. D.; Wang, W. Crystal growth pattern changes in low molecular weight poly(ethylene oxide) ultrathin films. *Polymer* **2011,** 52 (4), 1133-1140 DOI: https://doi.org/10.1016/j.polymer.2011.01.002.
61. Su, C.; Shi, G.; Wang, D.; Liu, G. A Model for the Crystal Orientation of Polymers Confined in 1D Nanocylinders. *Acta Polymerica Sinica* **2019**, DOI: doi: 10.11777/j.issn1000-3304.2018.18218.
62. Martin, J.; Mijangos, C.; Sanz, A.; Ezquerra, T. A.; Nogales, A. Segmental Dynamics of Semicrystalline Poly(vinylidene fluoride) Nanorods. *Macromolecules* **2009,** 42 (14), 5395-5401 DOI: 10.1021/ma900754v.
63. Vanroy, B.; Wübbenhorst, M.; Napolitano, S. Crystallization of thin polymer layers confined between two adsorbing walls. *ACS Macro Letters* **2013,** 2 (2), 168-172 DOI: 10.1021/mz300641x.
64. Napolitano, S.; Wübbenhorst, M. Slowing Down of the Crystallization Kinetics in Ultrathin Polymer Films: A Size or an Interface Effect? *Macromolecules* **2006,** 39 (18), 5967-5970 DOI: 10.1021/ma061304u.
65. Guan, Y.; Liu, G.; Ding, G.; Yang, T.; Mueller, A. J.; Wang, D. Enhanced Crystallization from the Glassy State of Poly(L-lactic acid) Confined in Anodic Alumina Oxide Nanopores. *Macromolecules* **2015,** 48 (8), 2526-2533 DOI: 10.1021/acs.macromol.5b00108.
66. Turnbull, D.; Fisher, J. C. Rate of Nucleation in Condensed Systems. *The Journal of Chemical Physics* **1949,** 17 (1), 71-73 DOI: 10.1063/1.1747055.
67. Forrest, J. A.; Dalnoki-Veress, K. The glass transition in thin polymer films. *Advances in Colloid and Interface Science* **2001,** 94 (1–3), 167-195 DOI: http://dx.doi.org/10.1016/S0001-8686(01)00060-4.
68. Li, L.; Zhou, D.; Huang, D.; Xue, G. Double Glass Transition Temperatures of Poly(methyl methacrylate) Confined in Alumina Nanotube Templates. *Macromolecules* **2014,** 47 (1), 297-303 DOI: 10.1021/ma4020017.
69. Li, L.; Chen, J.; Deng, W.; Zhang, C.; Sha, Y.; Cheng, Z.; Xue, G.; Zhou, D. Glass Transitions of Poly(methyl methacrylate) Confined in Nanopores: Conversion of Three- and

Two-Layer Models. *The Journal of Physical Chemistry B* **2015,** 119 (15), 5047-5054 DOI: 10.1021/jp511248q.
70. Wang, B.; Mathew, A.; Napolitano, S. Temperature and Thickness Dependence of the Time Scale of Crystallization of Polymers under 1D Confinement. *ACS Macro Letters* **2021,** 10 (4), 476-480 DOI: 10.1021/acsmacrolett.1c00123.
71. Casas, M. T.; Michell, R. M.; Blaszczyk-Lezak, I.; Puiggalí, J.; Mijangos, C.; Lorenzo, A. T.; Müller, A. J. Self-assembly of semicrystalline PE-b-PS diblock copolymers within AAO nanoporous templates. *Polymer* **2015,** 70, 282-289 DOI: https://doi.org/10.1016/j.polymer.2015.06.025.
72. Safari, M.; Martínez de Ilarduya, A.; Mugica, A.; Zubitur, M.; Muñoz-Guerra, S.; Müller, A. J. Tuning the Thermal Properties and Morphology of Isodimorphic Poly[(butylene succinate)-ran-(ε-caprolactone)] Copolyesters by Changing Composition, Molecular Weight, and Thermal History. *Macromolecules* **2018,** 51 (23), 9589-9601 DOI: 10.1021/acs.macromol.8b01742.
73. Safari, M.; Leon Boigues, L.; Shi, G.; Maiz, J.; Liu, G.; Wang, D.; Mijangos, C.; Müller, A. J. Effect of Nanoconfinement on the Isodimorphic Crystallization of Poly(butylene succinate-ran-caprolactone) Random Copolymers. *Macromolecules* **2020,** 53 (15), 6486-6497 DOI: 10.1021/acs.macromol.0c01081.
74. Pérez-Camargo, R. A.; Arandia, I.; Safari, M.; Cavallo, D.; Lotti, N.; Soccio, M.; Müller, A. J. Crystallization of isodimorphic aliphatic random copolyesters: Pseudo-eutectic behavior and double-crystalline materials. *European Polymer Journal* **2018,** 101, 233-247 DOI: https://doi.org/10.1016/j.eurpolymj.2018.02.037.